Effect of local E×B flow shear on the stability of magnetic islands in tokamak plasmas

R. Fitzpatrick and F. L. Waelbroeck

Department of Physics, Institute for Fusion Studies, University of Texas at Austin, Austin, Texas 78712, USA

The influence of local $\mathbf{E} \times \mathbf{B}$ flow shear on a relatively wide, constant-ψ, magnetic island embedded in a large-aspect-ratio, low-β, circular cross-section tokamak plasma is examined, using a slab approximation to model the magnetic geometry. It is found that there are *three* separate solution branches characterized by low, intermediate, and high values of the shear. Flow shear is found to have a *stabilizing* effect on island solutions lying on the low and high shear branches, via a nonlinear modification of the ion polarization term in the Rutherford island width evolution equation, but to have a *destabilizing* effect on solutions lying on the intermediate shear branch. Moreover, the effect is *independent* of the sign of the shear. The modification of island stability by local $\mathbf{E} \times \mathbf{B}$ flow shear is found to peak when the magnitude of the shear is approximately v_i/L_s, where v_i is the ion thermal velocity, and L_s the magnetic shear length. © *2009 American Institute of Physics.*
[DOI: 10.1063/1.3126964]

I. INTRODUCTION

A conventional magnetic confinement device is designed to trap a thermonuclear plasma on a set of toroidally nested magnetic flux surfaces.[1] Heat and particles *flow around* these surfaces relatively rapidly, due to the free streaming of charged particles along magnetic field lines, but are only able to *diffuse across* them relatively slowly, assuming that the particle gyroradii are much smaller than the minor radius of the device. A *tokamak* is a particularly successful type of magnetic confinement device which is *toroidally axisymmetric*, and whose magnetic field is dominated by an approximately uniform toroidal component.[2,3]

Tokamak plasmas are subject to a number of macroscopic instabilities which limit their effectiveness.[3,4] Among these, *tearing modes*[5,6] are comparatively slowly growing instabilities which eventually saturate,[7,8] in the process reconnecting magnetic flux surfaces to form *magnetic islands*.[1] These are radially localized helical structures which are centered on so-called *rational flux surfaces*: i.e., magnetic flux surfaces that satisfy $\mathbf{k} \cdot \mathbf{B} = 0$, where $\mathbf{k}$ is the wave number of the instability, and $\mathbf{B}$ the equilibrium magnetic field. Magnetic islands degrade plasma confinement because they enable heat and particles to flow rapidly along field-lines from their inner to their outer radii, implying an almost complete loss of confinement in the region lying between these radii.[9]

Tokamak plasmas are often heated by neutral beam injection (NBI),[2] which can be either *balanced*, such very little net toroidal momentum is injected into the plasma, or *unbalanced*, such that significant toroidal momentum is injected into the plasma. The DIII-D tokamak's[10] NBI system was recently reconfigured so as to enable either balanced or unbalanced operation (previously, only unbalanced operation had been possible). It was subsequently discovered that plasma discharges heated by unbalanced NBI tend to contain *narrower* magnetic islands than otherwise similar discharges heated by balanced NBI.[11] Of course, the former type of discharge is characterized by higher levels of plasma flow and flow shear than the latter. However, according to standard theory,[6] when considering the effect of plasma flow on an individual magnetic island, the local flow can always be *transformed away* by moving to a frame of reference which corotates with the island. On the other hand, the flow shear *cannot* be transformed away. Thus, a possible explanation for the relatively narrow magnetic islands observed in DIII-D discharges heated by unbalanced NBI is that they are *stabilized* by the comparatively high levels of flow shear present in such discharges. Of course, this explanation presupposes that flow shear generally has a stabilizing effect on magnetic islands.

In general, plasma flow (i.e., ion fluid flow) is made up of a combination of $\mathbf{E} \times \mathbf{B}$ flow, diamagnetic flow, and parallel (to the equilibrium magnetic field) flow.[12] It follows that flow shear is also made up of $\mathbf{E} \times \mathbf{B}$, diamagnetic, and parallel components. Now, the toroidal momentum injection associated with unbalanced NBI generates strong parallel flow shear (since the parallel direction is predominately toroidal), and much weaker $\mathbf{E} \times \mathbf{B}$ shear (since the $\mathbf{E} \times \mathbf{B}$ direction only has a small toroidal component). On the other hand, toroidal momentum injection does not directly generate diamagnetic flow shear. Of course, such shear may be produced by the plasma heating associated with NBI, but this effect should be more or less the same for balanced and unbalanced injection, and is therefore neglected in the following.

Now, there are *three* main mechanisms by which flow shear can affect the stability of a magnetic island. First, the shear in the *global* flow profile can modify the island's tearing stability index.[13–15] This effect is easily calculated from linear theory, and is generally found to be stabilizing for sufficiently strong flow shear.[13,14] Second, the shear in the *global* flow profile can suppress the mutually destabilizing interaction between the island and any other islands present in the plasma which couple to it via toroidicity, pressure, or

16, 052502-1

flux-surface shaping.[16,17] This effect can also be calculated from linear theory, and is obviously stabilizing. Third, the shear in the *local* flow profile can directly modify the plasma flow and current patterns in the immediate vicinity of the island.[18] This effect, which can only be calculated from nonlinear theory, is far less completely understood than the other two. It is predominately associated with $\mathbf{E} \times \mathbf{B}$ flow shear, since $\mathbf{E} \times \mathbf{B}$ flow generates an *ion polarization current* in the vicinity of the island, whereas parallel flow does not drive any such current. Hence, we shall concentrate on $\mathbf{E} \times \mathbf{B}$ flow shear in this paper.

The aim of this article is to extend some recent analytical work[19] in order to examine the effect of *local* $\mathbf{E} \times \mathbf{B}$ flow shear on magnetic island stability in a conventional large aspect-ratio, low-β, circular cross-section tokamak plasma. The analysis in question, which proceeds via a systematic expansion in small quantities, is based on the so-called *five-field model* of plasma dynamics,[20–22] which is a generalization of the well-known *four-field model* of Hazeltine *et al.*[23] The five-field model is derived using a low-β, drift-MHD ordering of plasma parameters.[12] It incorporates diamagnetic flows, ion gyroviscosity, fast parallel electron heat transport, the shear-Alfvén wave, the ion sound wave, and the drift wave.

In the following, for the sake of simplicity, we shall use a *slab approximation* to model the magnetic geometry. We shall also restrict our attention to *comparatively wide* magnetic islands (i.e., islands in the so-called subsonic, sonic, or supersonic regimes identified in Ref. 19).

II. ANALYSIS

A. Coordinates

Let us adopt the right-handed Cartesian coordinates x, y, z. Suppose that there is no variation of quantities in z-direction: i.e., $\partial / \partial z \equiv 0$. The system is assumed to be periodic in the y-direction, with periodicity length $2\pi/k$. Roughly speaking, the x-direction represents the radial direction, the y-direction the poloidal direction, and the z-direction the direction along the resonant magnetic field line.

B. Asymptotic matching

Consider a quasineutral tokamak plasma consisting of electrons and singly charged ions. The plasma is conveniently divided into an "inner region," which comprises the plasma in the immediate vicinity of the island, and an "outer region," which comprises the remainder of the plasma. Linear analysis is perfectly adequate in the outer region, whereas nonlinear analysis is generally required in the inner region.[6] As is well known, the five-field equations reduce to the much simpler *ideal-MHD* equations in the outer region.[5] Let us assume that a conventional linear ideal-MHD solution has been found in this region. The solution is characterized by a single parameter, Δ', defined as the jump in the logarithmic derivative of the x-component of the perturbed magnetic field across the inner region.[5] This parameter, which is known as the *tearing stability index*, measures the free en-

ergy available in the outer region to drive the tearing mode. The mode is destabilized if $\Delta' > 0$. It remains to obtain a nonlinear solution of the five-field equations in the inner region, and then to asymptotically match this solution to the aforementioned linear ideal-MHD solution at the boundary between the inner and the outer regions.

C. Unperturbed plasma equilibrium

The unperturbed (i.e., in the absence of the island) plasma equilibrium is assumed not to vary in the y-direction. The inner region is confined to a relatively thin layer, centered on the rational surface. In this region, the unperturbed equilibrium magnetic field takes the form

$$\mathbf{B} = B_z \left(\frac{x}{L_s} \mathbf{e}_y + \mathbf{e}_z \right), \tag{1}$$

where B_z is a uniform constant, and L_s the *magnetic shear length*. Likewise, the unperturbed equilibrium electron number density is written

$$n_e = n_{e0} \left(1 + \frac{x}{L_n} \right), \tag{2}$$

where n_{e0} is a uniform constant, and L_n the *density gradient scale length*. The unperturbed equilibrium electron temperature takes the form

$$T_e = T_{e0} \left(1 + \frac{x}{L_T} \right), \tag{3}$$

where T_{e0} is a uniform constant, and L_T the *electron temperature gradient scale length*. The unperturbed equilibrium $\mathbf{E} \times \mathbf{B}$ velocity is written

$$\mathbf{V}_{EB} = V_0 \left(1 + \frac{x}{L_V} \right) \mathbf{e}_y, \tag{4}$$

where V_0 is a uniform constant, and L_V the $\mathbf{E} \times \mathbf{B}$ *velocity gradient scale length*. Finally, for the sake of simplicity, the ion temperature is assumed to take the constant value T_i.

D. Tearing perturbation

Suppose that the plasma equilibrium is perturbed by a tearing instability which is periodic in the y-direction with wave number k. Note that $\mathbf{k} \cdot \mathbf{B} = 0$ at $x=0$. Hence, the rational surface lies at $x=0$. The instability is assumed to saturate to produce a thin (relative to the width of the plasma in the x-direction) magnetic island. The magnetic island is wholly contained within the inner region. Let the width of the island in the x-direction satisfy

$$w \ll L_s, \ L_n, \ L_T, \ L_V, \ k^{-1}. \tag{5}$$

Finally, suppose that the island propagates in the y-direction at some steady phase velocity V_p.

E. Plasma parameters

At this stage, it is helpful to define the following fundamental plasma parameters. First, the *electron beta*,

$$\beta = \frac{\mu_0 n_{e0} T_{e0}}{B_z^2}, \tag{6}$$

which is assumed to be much less than unity. Second, the *ion sound radius*,

$$\rho_s = \frac{\sqrt{T_{e0}/m_i}}{eB_z/m_i}, \tag{7}$$

which is assumed to be much less than the width of the inner region, and, therefore, much smaller than L_s, L_n, L_T, L_V, or k^{-1}. Here, e is the magnitude of the electron charge. Finally, the *electron diamagnetic velocity*,

$$V_* = \frac{T_{e0}}{eB_z L_n}, \tag{8}$$

which is assumed to be much less than the compressional Alfvén velocity.

It is also helpful to define the following dimensionless parameters. First, the *ion to electron temperature ratio*,

$$\tau = \frac{T_i}{T_{e0}}. \tag{9}$$

Second, the *ion sound parameter*,

$$\alpha = \sqrt{1+\tau} \frac{L_n}{L_s} \frac{w}{\rho_s}, \tag{10}$$

which determines whether the island is in the subsonic, sonic, or supersonic regimes identified in Ref. 19. In fact, the subsonic regime corresponds to $\alpha \gg 1$, the sonic regime to $\alpha \sim \mathcal{O}(1)$, and the supersonic regime to $L_n/L_s \ll \alpha \ll 1$. Finally, the *local $\mathbf{E} \times \mathbf{B}$ flow shear parameter*,

$$\sigma = \left. \frac{w}{V_*} \frac{dV_{EBy}}{dx} \right|_{x=0} = \frac{V_0}{V_*} \frac{w}{L_V}. \tag{11}$$

F. Orderings

Our analysis is based on the following ordering scheme:

$$L_n \ll L_s, \tag{12}$$

$$\beta \ll \left(\frac{L_n}{L_s}\right)^2 \left(\frac{w}{\rho_s}\right)^2, \tag{13}$$

$$\rho_s \ll w. \tag{14}$$

The first two orderings are fairly standard in a large aspect ratio, low-β, tokamak plasma, while the third implies that the island is relatively wide, so that it lies in the so-called *subsonic*, *sonic*, or *supersonic* regimes identified in Ref. 19, as opposed to the *hypersonic* regime. Furthermore, it is a fundamental assumption in our analysis that any perpendicular transport terms appearing in the five-field equations, such as resistivity and ion viscosity, are *very much smaller* than the leading terms in these equations.

G. Magnetic flux function

Let $\psi = A_z L_s/(B_z w^2)$, where A_z is the z-component of the magnetic vector potential. It is easily demonstrated that ψ is a magnetic flux function: i.e., $\mathbf{B} \cdot \nabla \psi = 0$. Moreover, ordering (13) ensures that the well-known constant-ψ approximation[5] is valid, so that

$$\psi(X, \theta) = -X^2/2 + \cos \theta, \tag{15}$$

where $X = x/w$ and $\theta = ky$. The above magnetic flux function maps out a magnetic island, centered on $x=0$. The O-point lies at $x=0$, $\theta=0$, and $\psi=+1$, whereas the X-point lies at $x=0$, $\theta=\pi$, and $\psi=-1$. The region lying inside the magnetic separatrix (which is situated at $\psi=-1$) corresponds to $+1 > \psi > -1$, whereas the region lying outside the separatrix corresponds to $-1 \geq \psi > -\infty$. Finally, the full island width in the x-direction is $4w$. Note that our fundamental assumption that any perpendicular transport terms appearing in the five-field equations are extremely small precludes the type of viscosity-induced distortions of magnetic island structure considered in Ref. 24.

H. Flux-surface average operator

The *flux-surface average operator* is defined as the annihilator of $\mathbf{B} \cdot \nabla A$ for any $A(x, \theta)$: i.e., $\langle \mathbf{B} \cdot \nabla A \rangle \equiv 0$. It is easily shown that

$$\langle f(s, \psi, \theta) \rangle = \oint \frac{f(s, \psi, \theta)}{\sqrt{2(-\psi + \cos \theta)}} \frac{d\theta}{2\pi} \tag{16}$$

outside the magnetic separatrix, and

$$\langle f(s, \psi, \theta) \rangle = \int_{-\theta_0}^{\theta_0} \frac{f(s, \psi, \theta) + f(-s, \psi, \theta)}{2\sqrt{2(-\psi + \cos \theta)}} \frac{d\theta}{2\pi} \tag{17}$$

inside the separatrix, where $s = \mathrm{sgn}(X)$, and $\theta_0 = \cos^{-1}(\psi)$.

I. Modified plasma equilibrium

As is demonstrated in Ref. 19, in the presence of a subsonic/sonic/supersonic magnetic island, the various equilibrium profiles take the form

$$\frac{L_n}{n_{e0}} \frac{\partial n_e}{\partial x} = XL, \tag{18}$$

$$\frac{L_T}{T_{e0}} \frac{\partial T_e}{\partial x} = XL, \tag{19}$$

$$\frac{V_{iy}}{V_*} = X(M + \tau L), \tag{20}$$

$$\frac{V_{EBy}}{V_*} = XM, \tag{21}$$

$$\frac{V_{ey}}{V_*} = X(M - L), \tag{22}$$

where V_{iy}, V_{EBy}, and V_{ey} are the y-components of the ion fluid, $\mathbf{E} \times \mathbf{B}$, and electron fluid velocities, respectively, in the

island rest frame. Moreover, L and M are both *flux-surface functions*: i.e., $L=L(s,\psi)$ and $M=M(s,\psi)$.

J. Profile functions

It is clear from Eqs. (18)–(22) that the modified equilibrium profiles are determined by the two profile functions $L(s,\psi)$ and $M(s,\psi)$. Indeed, the first function specifies the density and electron temperature profiles, while the second determines the $\mathbf{E}\times\mathbf{B}$ velocity profile. According to Ref. 19, in the subsonic/sonic/supersonic magnetic island regime, the first profile function takes the form

$$L(s,\psi) = \begin{cases} 0, & \psi > -1, \\ s/\langle X^2\rangle, & \psi \le -1. \end{cases} \tag{23}$$

It follows that the density and electron temperature profiles are *completely flattened* inside the island separatrix (i.e., for $\psi > -1$). The apparent discontinuity in $L(s,\psi)$ across the island separatrix is resolved by a thin boundary layer of thickness $\rho_s \ll w$.[25] Reference 19 also derives the following differential equation satisfied by the second profile function,

$$0 = \frac{d}{d\psi}\left[\frac{d(M+\tau L)}{d\psi}\langle X^4\rangle + \zeta\left(\frac{[M(L-M)\tau/2]L'}{M(L-M)+\alpha^2}\right)\langle\widetilde{X^2 X^2}\rangle\right]$$
$$- \zeta\left(\frac{M[M'+\tau(L'+M')/2]L'}{M(L-M)+\alpha^2}\right)\langle\widetilde{X^2 X^2}\rangle, \tag{24}$$

with $' \equiv d/d\psi$, and $\tilde{A} \equiv A - \langle A\rangle/\langle 1\rangle$. Here,

$$\zeta = \frac{\beta(\eta_\parallel/\mu_0)+(\kappa_{\perp e}/n_{e0})}{(\mu_{\perp i}/n_{e0}m_i)}, \tag{25}$$

where $\eta_\parallel$, $\kappa_{\perp e}$, and $\mu_{\perp i}$ are the parallel resistivity, perpendicular electron heat conductivity, and perpendicular ion viscosity, respectively. Note that ζ is the ratio of the effective perpendicular particle diffusivity to the perpendicular ion momentum diffusivity.

K. Boundary conditions

Within the separatrix, Eq. (24) simplifies considerably to give

$$0 = \frac{d}{d\psi}\left[\frac{dM}{d\psi}\langle X^4\rangle\right]. \tag{26}$$

The only solution to this equation which is well-behaved at the island O-point is

$$M = m_0, \tag{27}$$

where m_0 is a constant.

Far from the island, Eq. (24) is subject to the boundary condition

$$M(\pm 1,\psi\to -\infty) \to -\frac{sv_{\infty\pm}}{\sqrt{-2\psi}} + \sigma, \tag{28}$$

where $v_{\infty\pm}$ are constants, and use has been made of Eqs. (11) and (21). Incidentally, the above boundary condition ensures that the island is subject to *zero net electromagnetic torque* (due, for instance, to interaction with a resistive wall or an error field).[26]

It is helpful to define

$$v_\infty = (v_{\infty+} + v_{\infty-})/2. \tag{29}$$

This parameter determines the effective island phase velocity, V_p, relative to the unperturbed $\mathbf{E}\times\mathbf{B}$ velocity at the rational surface, V_0, according to the relation

$$V_p = V_0 + v_\infty V_*. \tag{30}$$

Here, V_* is the (magnitude of the) electron diamagnetic velocity. (The ion diamagnetic velocity is τV_*). Thus, $v_\infty = -1$, 0, τ corresponds to the island propagating with the unperturbed local electron, $\mathbf{E}\times\mathbf{B}$, or ion fluid, respectively.

L. Momentum conservation

Equation (24) ensures the conservation of the ion momentum flux from magnetic flux surface to magnetic flux surface. In general, the form of this equation is complicated because, in addition to the standard viscous ion momentum flux, there are also momentum fluxes associated with Reynolds stresses and ion gyroviscous stresses. However, there are two limits in which the ion momentum flux becomes relatively simple.

Far from the island (i.e., $|X| \gg 1$), the Reynolds stresses and ion gyroviscous stresses (which all depend on L') are negligible, and the ion momentum flux becomes predominately viscous. In this limit, the normalized ion momentum flux (in the x-direction) is written

$$\Gamma_{i\pm} = \left.\frac{w}{V_*}\frac{dV_{iy}}{dx}\right|_{X\to\pm\infty}$$
$$= M(\pm 1,\psi\to -\infty) + \tau L(\pm 1,\psi\to\infty) = \sigma, \tag{31}$$

where use has been made of Eqs. (20), (23), and (28).

Inside the island separatrix, the Reynolds stresses and ion gyroviscous stresses are zero (since $L'=0$), and the ion momentum flux is purely viscous. Thus, the normalized ion momentum flux across the rational surface (which lies entirely within the island separatrix) is

$$\Gamma_{i0} = \left.\frac{w}{V_*}\frac{dV_{yi}}{dx}\right|_{X=0} = m_0, \tag{32}$$

where use has been made of Eqs. (20), (23), and (27).

Now, a fundamental assumption in all of our analysis is that we are searching for a *steady-state* island solution. We expect such a solution to possess a *fully relaxed* ion velocity profile characterized by

$$\Gamma_{i-} = \Gamma_{i0} = \Gamma_{i+}, \tag{33}$$

since if this is not the case then ion momentum will gradually accumulate in the island region, causing the ion velocity profile to evolve in time. Thus, we conclude from Eqs. (31) and (32) that

$$m_0 = \sigma. \tag{34}$$

In other words, in a steady-state solution, the $\mathbf{E}\times\mathbf{B}$ velocity shear inside the island separatrix matches the local unperturbed (by the island) equilibrium $\mathbf{E}\times\mathbf{B}$ velocity shear. Incidentally, the constraint (33) rules out the obviously unre-
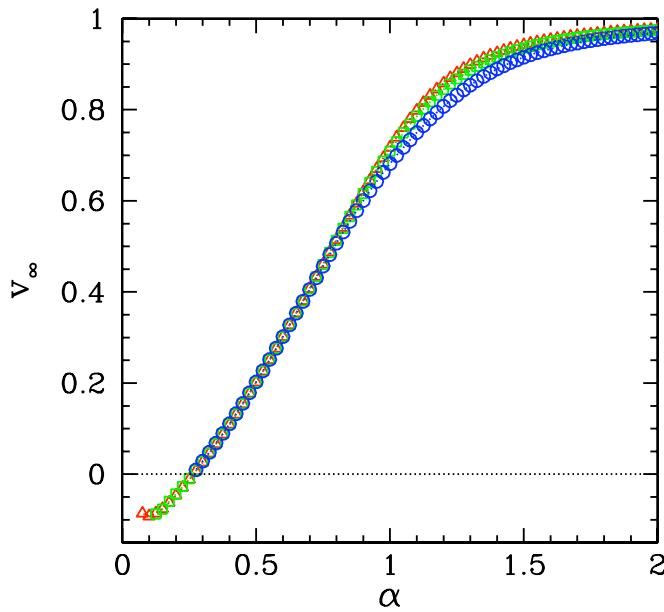
FIG. 1. (Color online) The island phase velocity parameter, v_∞, calculated as a function of the sound wave parameter, α, for $\tau=1.0$, $\zeta=1.0$, and $\epsilon=10^{-3}$. The red (triangle), green (square), and blue (circle) curves correspond to $|\sigma|=0.0$, 0.1, and 0.2, respectively.
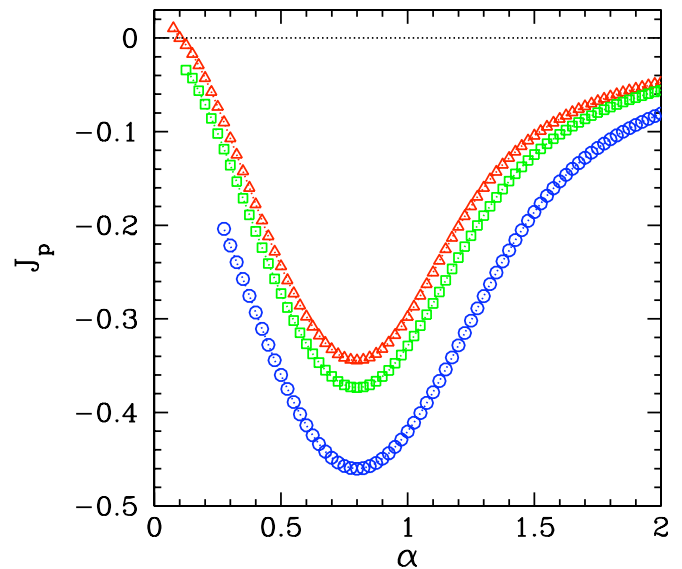

FIG. 2. (Color online) The ion polarization parameter, J_p, calculated as a function of the sound wave parameter, α, for $\tau=1.0$, $\zeta=1.0$, and $\epsilon=10^{-3}$. The red (triangle), green (square), and blue (circle) curves correspond to $|\sigma|=0.0$, 0.1, and 0.2, respectively.

laxed **E** × **B** velocity profiles considered in Ref. 27.[18]

M. Rutherford equation

Asymptotic matching between the solutions in the inner and outer regions yields the Rutherford island width evolution equation,[6]

$$\frac{dw}{dt} \propto \Delta' \rho_s + J_p \beta \left(\frac{L_s}{L_n}\right)^2 \left(\frac{\rho_s}{w}\right)^3, \tag{35}$$

where Δ' is the linear tearing stability index,[5] and

$$J_p = 2 \int_1^{-\infty} [\{M(M+\tau L)/2\}_+]' \langle \widetilde{X^2}\widetilde{X^2} \rangle d\psi. \tag{36}$$

Here, $F_+(\psi) \equiv [F(1,\psi)+F(-1,\psi)]/2$, assuming that $F \equiv F(s,\psi)$. The first term on the right-hand side of Eq. (35) parameterizes the contribution to the free energy available to drive the growth of the magnetic island which originates from the outer region, whereas the second parametrizes the corresponding contribution which originates from the inner region. The latter is usually ascribed to the *ion polarization current*.[28] It follows that local **E** × **B** flow shear can affect island stability by modifying either the linear tearing stability index, or the nonlinear ion polarization term, in the Rutherford equation. This article is focused on the latter mechanism.

N. Parity

Equation (24) is invariant under the parity transformation $s \rightarrow -s$, $M \rightarrow -M$. Thus, it follows from Eqs. (28), (29), and (36) that $\sigma \rightarrow -\sigma$, $v_\infty \rightarrow v_\infty$, and $J_p \rightarrow J_p$ under such a transformation. We conclude that the island phase velocity (relative to the unperturbed **E** × **B** velocity at the rational surface) and ion polarization contribution to the Ruther-

equation only depend on the *magnitude* of the local **E** × **B** flow shear parameter, σ, and are independent of its sign: i.e., v_∞ and J_p are functions of $|\sigma|$. Of course, the island phase velocity and the ion polarization contribution are both completely independent of the local **E** × **B** velocity, V_0 [see Eq. (4)], which transforms away in the island rest frame.

III. RESULTS

A. Introduction

The full details of how the island phase velocity parameter, v_∞, and the ion polarization parameter, J_p, are calculated as functions of the sound wave parameter, α, and the local **E** × **B** flow shear parameter, σ, are given in Appendix. In discussing our results, it is convenient to make a distinction between the *low flow shear limit*, $|\sigma| \ll \alpha$, the *intermediate flow shear limit*, $|\sigma| \sim \mathcal{O}(\alpha)$, and the *high flow shear limit*, $|\sigma| \gg \alpha$.

B. Low flow shear

The typical behavior in the low flow shear limit, $|\sigma| \ll \alpha$, is illustrated in Figs. 1 and 2.

It can be seen from Fig. 1 that in the subsonic regime, $\alpha \gg 1$, the island phase velocity matches the local ion fluid velocity (i.e., $v_\infty \simeq \tau$), whereas in the supersonic regime, $\alpha \ll 1$, the phase velocity is close to the local **E** × **B** fluid velocity (i.e., $v_\infty \simeq 0$), and, finally, in the sonic regime, $\alpha \sim \mathcal{O}(1)$, it lies somewhere between these two velocities.[19] Furthermore, it is clear from Fig. 2 that the ion polarization term in the Rutherford equation is *stabilizing* (i.e., $J_p < 0$). The magnitude of this term peaks in the sonic regime, and is comparatively small in the subsonic and supersonic regimes.[19]

According to Fig. 1, relatively low amounts of local **E** × **B** flow shear cause the island phase velocity to shift
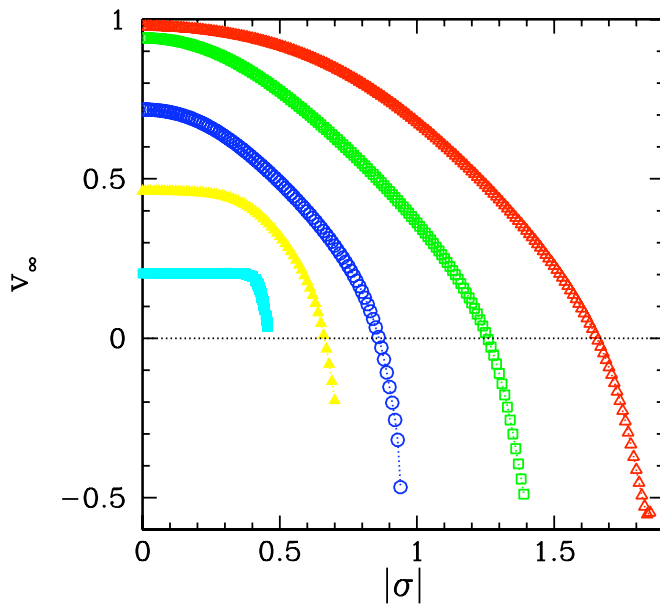
FIG. 3. (Color online) The island phase velocity parameter, v_∞, calculated as a function of the local $\mathbf{E} \times \mathbf{B}$ flow shear parameter, σ, for $\tau=1.0$, $\zeta=1.0$, and $\epsilon=10^{-2}$. The red (open triangle), green (open square), blue (open circle), yellow (solid triangle), and cyan (solid square) curves correspond to $\alpha=2.0$, 1.5, 1.0, 0.75, and 0.5, respectively.

FIG. 4. (Color online) The ion polarization parameter, J_p, calculated as a function of the local $\mathbf{E} \times \mathbf{B}$ flow shear parameter, σ, for $\tau=1.0$, $\zeta=1.0$, and $\epsilon=10^{-2}$. The red (open triangle), green (open square), blue (open circle), yellow (solid triangle), and cyan (solid square) curves correspond to $\alpha=2.0$, 1.5, 1.0, 0.75, and 0.5, respectively.

slightly in the electron diamagnetic direction (i.e., it makes v_∞ more negative). Moreover, it can be seen from Fig. 2 that low local $\mathbf{E} \times \mathbf{B}$ flow shear has a *stabilizing* effect on the island (i.e., it makes J_p more negative). The magnitude of this stabilizing effect clearly peaks in the sonic regime.

C. Low to moderate flow shear

The typical behavior in the low to moderate flow shear limit, $0 < |\sigma| \lesssim \alpha$, is illustrated in Figs. 3 and 4.

According to Fig. 3, as the local $\mathbf{E} \times \mathbf{B}$ flow shear increases from a relatively low value, it generates an increasingly large phase velocity shift, toward the electron diamagnetic direction, in island solutions lying on the low flow shear branch. Eventually, when $|\sigma| \simeq 0.85\alpha$, the direction of island propagation in the local $\mathbf{E} \times \mathbf{B}$ frame (at the rational surface) switches from the ion to the electron diamagnetic direction (i.e., v_∞ becomes negative). Finally, the low flow shear solution branch ceases to exist when $|\sigma| \simeq \alpha$.

It can be seen from Fig. 4 that islands on the low flow shear solution branch become *more stable* (i.e., J_p becomes more negative) as the local $\mathbf{E} \times \mathbf{B}$ flow shear increases. This flow shear stabilization effect *peaks* just before the switch in direction of island propagation in the local $\mathbf{E} \times \mathbf{B}$ frame. Furthermore, the effect increases monotonically with increasing α, and so is smallest in the supersonic regime, and largest in the subsonic regime.

D. High flow shear

The typical behavior in the high flow shear limit, $|\sigma| \gg \alpha$, is illustrated in Figs. 5 and 6.

It can be seen from Fig. 5 that at high levels of local $\mathbf{E} \times \mathbf{B}$ flow shear there exists a branch of island solutions which propagate in the *ion diamagnetic direction* relative to
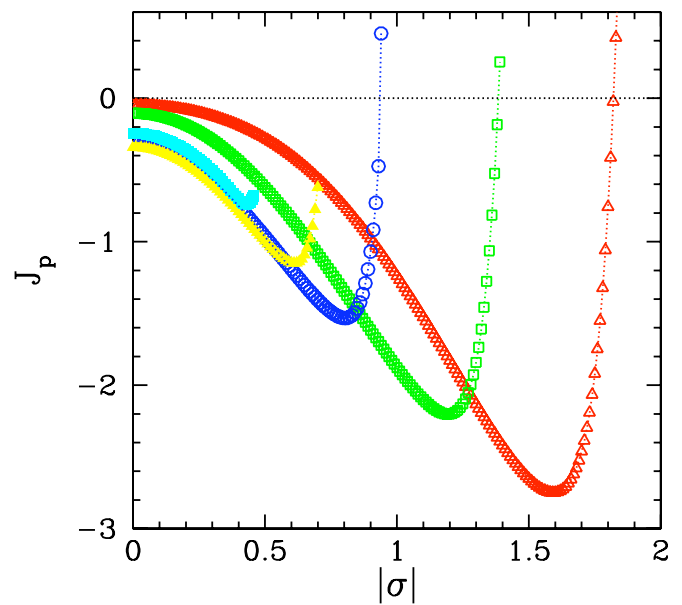
the local ion fluid frame (i.e., which have $v_\infty > \tau$). Moreover, the island phase velocity shifts in the electron diamagnetic direction as the local $\mathbf{E} \times \mathbf{B}$ flow shear increases in magnitude, although the shift becomes increasingly small as $|\sigma| \to \infty$, and is never sufficient to reverse the direction of island propagation in the local ion fluid frame (i.e., v_∞ always remains greater than τ). Finally, the high flow shear solution
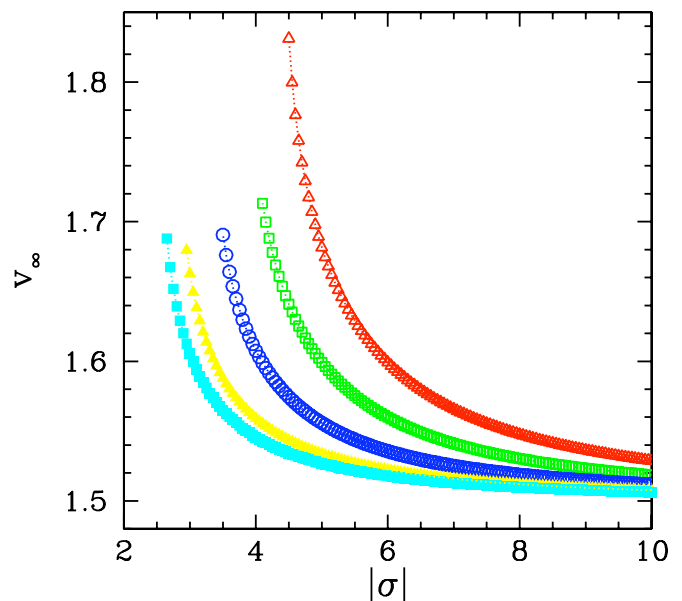

FIG. 5. (Color online) The island phase velocity parameter, v_∞, calculated as a function of the local $\mathbf{E} \times \mathbf{B}$ flow shear parameter, σ, for $\tau=1.0$, $\zeta=1.0$, and $\epsilon=10^{-2}$. The red (open triangle), green (open square), blue (open circle), yellow (solid triangle), and cyan (solid square) curves correspond to $\alpha=2.0$, 1.5, 1.0, 0.5, and 0.0, respectively.
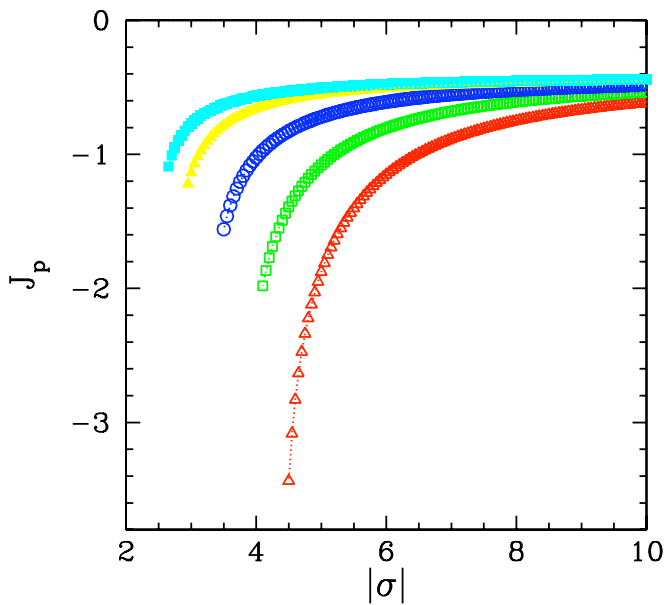
FIG. 6. (Color online) The ion polarization parameter, J_p, calculated as a function of the local **E** × **B** flow shear parameter, σ, for $\tau=1.0$, $\zeta=1.0$, and $\epsilon=10^{-2}$. The red (open triangle), green (open square), blue (open circle), yellow (solid triangle), and cyan (solid square) curves correspond to $\alpha=2.0$, 1.5, 1.0, 0.5, and 0.0, respectively.

branch ceases to exist below some critical flow shear which decreases with decreasing α.

According to Fig. 6, local **E** × **B** flow shear *stabilizes* (i.e., $J_p<0$) islands lying on the high flow shear solution branch. This effect is largest in the subsonic regime, and smallest in the supersonic regime. Furthermore, it decreases with increasing flow shear, but remains *finite* in the limit $|\sigma|\to\infty$.

E. Intermediate flow shear

We have seen that there is a *low flow shear branch* of island solutions which disappears when $|\sigma|$ exceeds α (see Figs. 3 and 4), and a *high flow shear branch* that ceases to exist when $|\sigma|$ falls below some critical value which is somewhat larger than α (see Figs. 5 and 6). It turns out that there is an *intermediate flow shear branch* of island solutions which connects the low and high flow shear branches. This is illustrated in Figs. 7 and 8. It can be seen that there is a discontinuous bifurcation between the low and intermediate flow shear branches of island solutions when $|\sigma|\simeq\alpha$, whereas the intermediate and high flow shear solution branches merge smoothly at some critical value of $|\sigma|$ which exceeds α. Island solutions on the intermediate flow shear branch propagate in the *ion diamagnetic direction* in the local **E** × **B** frame (i.e., $v_\infty>0$), and are, for the most part, *destabilized* by local **E** × **B** flow shear (i.e., $J_p>0$).

IV. CONCLUSIONS

We have examined the influence of local **E** × **B** flow shear on a relatively wide, constant-ψ, magnetic island embedded in a large aspect-ratio, low-β, circular cross-section tokamak plasma, using a slab approximation to model the magnetic geometry. We find that there are *three* separate so-

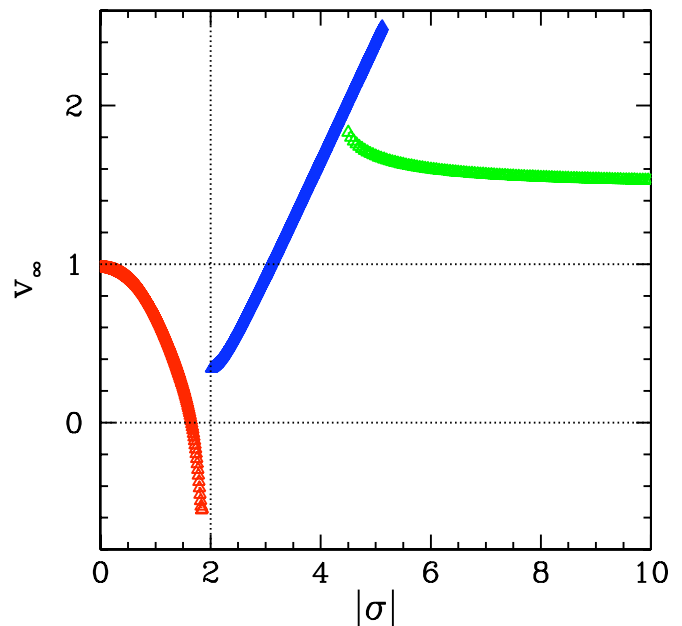FIG. 7. (Color online) The island phase velocity parameter, v_∞, calculated as a function of the local **E** × **B** flow shear parameter, σ, for $\alpha=2.0$, $\tau=1.0$, $\zeta=1.0$, and $\epsilon=10^{-2}$. The red (left), blue (middle), and green (right) curves correspond to the weak, intermediate, and strong flow shear regimes, respectively.

lution branches characterized by low, intermediate, and high values of the shear. Flow shear is found to have a *stabilizing* effect on island solutions lying on the low and high shear branches, via a nonlinear modification of the ion polarization term in the Rutherford island width evolution equation, but to have a generally *destabilizing* effect on solutions lying on the intermediate shear branch. Moreover, the effect is *independent* of the sign of the shear. The modification of island
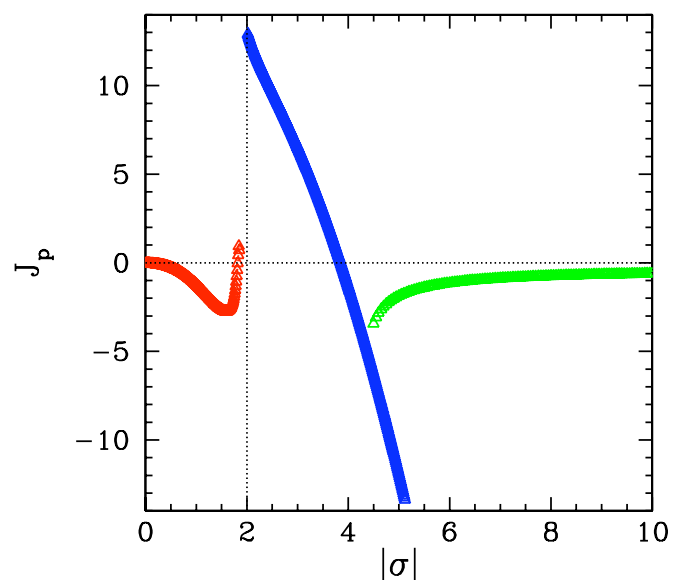

FIG. 8. (Color online) The ion polarization parameter, J_p, calculated as a function of the local **E** × **B** flow shear parameter, σ, for $\alpha=2.0$, $\tau=1.0$, $\zeta=1.0$, and $\epsilon=10^{-2}$. The red (left), blue (middle), and green (right) curves correspond to the weak, intermediate, and strong flow shear regimes, respectively.

stability by local $\mathbf{E} \times \mathbf{B}$ flow shear peaks when the magnitude of the shear is approximately v_i/L_s, where $v_i = \sqrt{T_{i0}/m_i}$ is the ion thermal velocity, and L_s the magnetic shear length. (This criterion corresponds to $|\sigma| \sim \alpha$.)

Our main conclusion, that local $\mathbf{E} \times \mathbf{B}$ velocity shear generally has a *stabilizing* effect on magnetic islands, is in accordance with the results of numerical simulations performed by Ofman and Morrison,[29] and Chen *et al.*[30] Interestingly, Chandra *et al.*[17] recently performed other simulations which suggest that local *parallel* velocity shear may have a *destabilizing* effect on magnetic islands. This result suggests that it may be worthwhile to extend the analysis presented here in order to take parallel velocity shear into account.

ACKNOWLEDGMENTS

APPENDIX A: CALCULATION DETAILS

1. Flux-surface functions

It is helpful to define the flux-surface label $k = \sqrt{(1-\psi)/2}$. It follows that $k=0$ at the island O-point, $k=1$ at the X-point, and $k \to \infty$ as $|X| \to \infty$. It is also helpful to define the complete elliptic integrals

$$E(l) = \int_0^{\pi/2} (1 - l^2 \sin^2 \varphi)^{1/2} d\varphi, \tag{A1}$$

$$K(l) = \int_0^{\pi/2} (1 - l^2 \sin^2 \varphi)^{-1/2} d\varphi. \tag{A2}$$

It is easily demonstrated that $E(0) = K(0) = \pi/2$, $E(1) = 1$, and $K \to \infty$ as $k \to 1$. Furthermore,

$$\langle 1 \rangle = \begin{cases} K(k)/\pi, & k < 1, \\ K(1/k)/k\pi, & k \ge 1, \end{cases} \tag{A3}$$

$$\langle X^2 \rangle = \begin{cases} (4/\pi)[(k^2-1)K(k) + E(k)], & k < 1, \\ (4/\pi)kE(1/k), & k \ge 1, \end{cases} \tag{A4}$$

$$\langle X^4 \rangle = \begin{cases} (16/3\pi)[(3k^4 - 5k^2 + 2)K(k) + 2(2k^2-1)E(k)], \\ \quad k < 1, \\ (16/3\pi)k^3[2(2-1/k^2)E(1/k) - (1-1/k^2)K(1/k)], \\ \quad k \ge 1. \end{cases} \tag{A5}$$

Finally, we can write

$$A(k) = \frac{\langle X^4 \rangle}{4k}, \tag{A6}$$

$$B(k) = \frac{\langle \widetilde{X^2}\widetilde{X^2} \rangle}{4k} = \frac{\langle X^4 \rangle - \langle X^2 \rangle^2/\langle 1 \rangle}{4k}. \tag{A7}$$

It is readily shown that $A(k) \to k^3$ as $k \to 0$, and $A(1) = B(1) = 8/3\pi$, plus $A(k) \to k^2$, $B(k) \to k^{-2}$ as $k \to \infty$.

2. Definitions

Let

$$L(s=1,k) \equiv L(k) = \frac{\pi}{4} \frac{1}{k} \frac{1}{E(1/k)} \tag{A8}$$

for $k \ge 1$, and

$$M(s,k) \equiv \begin{cases} M_0(k), & k < 1, \\ M_+(k), & k \ge 1, \ s = 1, \\ M_-(k), & k \ge 1, \ s = -1. \end{cases} \tag{A9}$$

3. Inside separatrix

Inside the separatrix (i.e., $0 \le k < 1$), Eq. (24) reduces to

$$\frac{d}{dk}\left[\frac{dM_0}{dk} A(k)\right] = 0. \tag{A10}$$

The only solution which is well behaved as $k \to 0$, and is consistent with a steady-state island solution (see Sec. II L), is

$$M_0 = \sigma. \tag{A11}$$

This solution corresponds to viscously relaxed *circulation* around island flux surfaces within the separatrix.

4. Separatrix

In the immediate vicinity of the separatrix, we can resolve the discontinuity in the profile function $L(k)$ by writing

$$L(y) \simeq \frac{\pi}{4}(1 - e^{-y}) \tag{A12}$$

for $y \ge 0$, where $y = (k-1)/\delta$, and $\delta \sim \rho_s/w \ll 1$. To lowest order in δ, Eq. (24) reduces to

$$0 = \frac{d}{dy}\left[\frac{d(M_\pm \pm \tau L)}{dy} \pm \zeta\left(\frac{[M_\pm(\pm L - M_\pm)\tau/2]L'}{M_\pm(\pm L - M_\pm) + \alpha^2}\right)\right]$$
$$\mp \zeta\left(\frac{M_\pm[M_\pm' + (\pm L' + M_\pm')\tau/2]L'}{M_\pm(\pm L - M_\pm) + \alpha^2}\right), \tag{A13}$$

where $' \equiv d/dy$. Potential singularities are avoided by letting

$$\frac{1}{M_\pm(\pm L - M_\pm) + \alpha^2} \to \frac{M_\pm(\pm L - M_\pm) + \alpha^2}{[M_\pm(\pm L - M_\pm) + \alpha^2]^2 + \epsilon^2}, \tag{A14}$$

where $\epsilon \ll 1$. The boundary conditions are

$$M_{\pm}(y=0) = \sigma, \tag{A15}$$

$$M'_{\pm}(y \to \infty) = 0. \tag{A16}$$

Equations (A13)–(A16) can be solved to give the parameters

$$m_{\pm} \equiv M_{\pm}(y \to \infty). \tag{A17}$$

Clearly, m_{+} represents the value of the profile function $M(s,k)$ immediately outside the separatrix, in the region $x > 0$, whereas m_{-} represents the corresponding value in the region $x < 0$. In general, $m_{+} \neq m_{-} \neq \sigma$. Thus, the profile function $M(s,k)$ is *discontinuous* across the island separatrix ($k = 1$). Note, however, that this discontinuity is entirely driven by the corresponding discontinuity in the profile function $L(s,k)$.

5. Outside separatrix

Outside the separatrix (i.e., $k \geq 1$), Eq. (24) reduces to

$$0 = \frac{d}{dk}\left[\frac{d(M_{\pm} \pm \tau L)}{dk} A(k) \right.$$
$$\left. \pm \zeta \left(\frac{[M_{\pm}(\pm L - M_{\pm})\tau/2]L'}{M_{\pm}(\pm L - M_{\pm}) + \alpha^2} \right) B(k) \right]$$
$$\mp \zeta \left(\frac{M_{\pm}[M'_{\pm} + (\pm L' + M'_{\pm})\tau/2]L'}{M_{\pm}(\pm L - M_{\pm}) + \alpha^2} \right) B(k), \tag{A18}$$

where $' \equiv d/dk$, and $L(k)$ is specified in Eq. (A8). Potential singularities are again avoided via the regularization procedure outlined in Eq. (A14). The boundary conditions are

$$M_{\pm}(0) = m_{\pm}, \tag{A19}$$

$$M_{\pm}(\infty) = \sigma. \tag{A20}$$

Equations (A18)–(A20) can be solved to give the profile functions $M_{\pm}(k)$ for $k \geq 1$, as well as the parameters

$$v_{\infty \pm} = \mp \lim_{k \to \infty} 2k(M_{\pm} - \sigma). \tag{A21}$$

6. Phase velocity parameter

The island phase velocity parameter, v_{∞}, is obtained from

$$v_{\infty} = (v_{\infty +} + v_{\infty -})/2. \tag{A22}$$

7. Ion polarization parameter

The ion polarization parameter, J_p, is given by

$$J_p = \left(\frac{16}{3\pi} \right)[m_{+}(m_{+} + \tau\pi/4) - \sigma^2]$$
$$+ \left(\frac{16}{3\pi} \right)[m_{-}(m_{-} - \tau\pi/4) - \sigma^2]$$
$$+ \int_1^{\infty} 2k[M'_{+}(M_{+} + \tau L) + M_{+}(M'_{+} + \tau L')]B(k)dk$$
$$+ \int_1^{\infty} 2k[M'_{-}(M_{-} - \tau L) + M_{-}(M'_{-} - \tau L')]B(k)dk, \tag{A23}$$

where $' \equiv d/dk$, and $L(k)$ is specified in Eq. (A8).

[1] A. H. Boozer, Rev. Mod. Phys. **76**, 1071 (2005).
[2] J. A. Wesson, *Tokamaks*, 3rd ed. (Oxford University Press, New York, 2004).
[3] J. P. Freidberg, *Ideal Magnetohydrodynamics* (Springer, New York, 1987).
[4] J. A. Wesson, Nucl. Fusion **18**, 87 (1978).
[5] H. P. Furth, J. Killeen, and M. N. Rosenbluth, Phys. Fluids **6**, 459 (1963).
[6] P. H. Rutherford, Phys. Fluids **16**, 1903 (1973).
[7] F. Militello and F. Porcelli, Phys. Plasmas **11**, L13 (2004).
[8] D. F. Escande and M. Ottaviani, Phys. Lett. A **323**, 278 (2004).
[9] Z. Chang and J. D. Callen, Nucl. Fusion **30**, 219 (1990).
[10] J. L. Luxon, Nucl. Fusion **42**, 614 (2002).
[11] R. J. Buttery, R. J. La Haye, P. Gohil, G. L. Jackson, H. Reimerdes, and E. J. Strait, and the DIII-D Team, Phys. Plasmas **15**, 056115 (2008).
[12] R. D. Hazeltine and J. D. Meiss, *Plasma Confinement* (Dover, New York, 2003).
[13] X. L. Chen and P. J. Morrison, Phys. Fluids B **2**, 495 (1990).
[14] X. L. Chen and P. J. Morrison, Phys. Fluids B **2**, 2575 (1990).
[15] D. Chandra, A. Sen, P. Kaw, M. P. Bora, and S. Kruger, Nucl. Fusion **45**, 524 (2005).
[16] R. Fitzpatrick, R. J. Hastie, T. J. Martin, and C. M. Roach, Nucl. Fusion **33**, 1533 (1993).
[17] D. Chandra, A. Sen, and P. Kaw, Nucl. Fusion **47**, 1238 (2007).
[18] F. L. Waelbroeck, R. Fitzpatrick, and D. Grasso, Phys. Plasmas **14**, 022302 (2007).
[19] R. Fitzpatrick and F. L. Waelbroeck, Phys. Plasmas **15**, 012502 (2008).
[20] A. Zeiler, J. F. Drake, and B. Rogers, Phys. Plasmas **4**, 2134 (1997).
[21] D. Grasso, M. Ottaviani, and F. Porcelli, Nucl. Fusion **42**, 1067 (2002).
[22] F. L. Waelbroeck, Phys. Rev. Lett. **95**, 035002 (2005).
[23] R. D. Hazeltine, M. Kotschenreuther, and P. J. Morrison, Phys. Fluids **28**, 2466 (1985).
[24] C. Ren, M. S. Chu, and J. D. Callen, Phys. Plasmas **6**, 1203 (1999).
[25] J. W. Connor, F. L. Waelbroeck, and H. R. Wilson, Phys. Plasmas **8**, 2835 (2001).
[26] F. L. Waelbroeck and R. Fitzpatrick, Phys. Rev. Lett. **78**, 1703 (1997).
[27] A. I. Smolyakov, E. Lazzaro, R. Coelho, and T. Ozeki, Phys. Plasmas **9**, 371 (2002).
[28] A. I. Smolyakov, Plasma Phys. Controlled Fusion **35**, 657 (1993).
[29] L. Ofman and P. J. Morrison, Phys. Fluids B **5**, 376 (1993).
[30] Q. Chen, A. Otto, and L. C. Lee, J. Geophys. Res. **102**, 151, DOI:10.1029/96JA03144 (1997).